17. J. Haywood, *The Penguin Historical Atlas of the Vikings* (Penguin Books, London, 1995).
18. N. A. Rosenberg *et al.*, *Genetics* **159**, 699 (2001).
19. J. L. Weber, K. W. Broman, *Adv. Genet.* **42**, 77 (2001).
20. A. R. Rogers, L. B. Jorde, *Am. J. Hum. Genet.* **58**, 1033 (1996).
21. M. Urbanek, D. Goldman, J. C. Long, *Mol. Biol. Evol.* **13**, 943 (1996).
22. J. F. Wilson *et al.*, *Nature Genet.* **29**, 265 (2001).
23. N. Risch, E. Burchard, E. Ziv, H. Tang, *Genome Biol.* **3**, comment2007.1 (2002).
24. D. C. Thomas, J. S. Witte, *Cancer Epidemiol. Biomark. Prev.* **11**, 505 (2002).
25. S. Wacholder, N. Rothman, N. Caporaso, *Cancer Epidemiol. Biomark. Prev.* **11**, 513 (2002).
26. J. K. Pritchard, P. Donnelly, *Theor. Popul. Biol.* **60**, 227 (2001).
27. S. E. Ptak, M. Przeworski, *Trends Genet.* **18**, 559 (2002).
28. L. Jin, R. Chakraborty, *Heredity* **74**, 274 (1995).
29. F. Calafell *et al.*, *Eur. J. Hum. Genet.* **6**, 38 (1998).
30. D. Altshuler, M. Cho, D. Falush, H. Innan, L. Kurina, J. Mountain, D. Nettle, M. Nordborg, M. Przeworski, N. Risch, D. Rosenberg, M. Stephens, D. Thomas, and E. Ziv provided helpful comments. The Mammalian Genotyping Service is supported by the National Heart, Lung, and Blood Institute. This work was supported by an NSF Biological Informatics Postdoctoral Fellowship (N.A.R.), a Burroughs-Wellcome Fund Hitchings Elion grant (J.K.P.), and NIH GM28428 (M.W.F.).

Supporting Online Material
www.sciencemag.org/cgi/content/full/298/5602/2381/DC1
Materials and Methods
Supporting Text
Figs. S1 and S2
Tables S1 to S4
References

19 June 2002; accepted 30 October 2002

NPAS2: A Gas-Responsive Transcription Factor

Elhadji M. Dioum,[1] Jared Rutter,[2] Jason R. Tuckerman,[1] Gonzalo Gonzalez,[1] Marie-Alda Gilles-Gonzalez,[1]* Steven L. McKnight[2]*

Neuronal PAS domain protein 2 (NPAS2) is a mammalian transcription factor that binds DNA as an obligate dimeric partner of BMAL1 and is implicated in the regulation of circadian rhythm. Here we show that both PAS domains of NPAS2 bind heme as a prosthetic group and that the heme status controls DNA binding in vitro. NPAS2-BMAL1 heterodimers, existing in either the apo (heme-free) or holo (heme-loaded) state, bound DNA avidly under favorably reducing ratios of the reduced and oxidized forms of nicotinamide adenine dinucleotide phosphate. Low micromolar concentrations of carbon monoxide inhibited the DNA binding activity of holo-NPAS2 but not that of apo-NPAS2. Upon exposure to carbon monoxide, inactive BMAL1 homodimers were formed at the expense of NPAS2-BMAL1 heterodimers. These results indicate that the heterodimerization of NPAS2, and presumably the expression of its target genes, are regulated by a gas through the heme-based sensor described here.

PAS domains are independently folding modules of ~130 amino acids that detect diverse environmental signals, including oxygen, light, voltage, redox potential, and many small aromatic molecules (*1*–*7*). Although these domains have modest sequence similarity, they share strikingly similar three-dimensional folds (*8*–*12*). Two groups of bacterial proteins—the FixL proteins of *Rhizobia* and the PDEA1 phosphodiesterases of *Acetobacter*—use heme bound within a PAS domain to sense oxygen (*13*). In FixL, binding of oxygen to the heme controls a kinase domain that phosphorylates a cognate transcription factor. In PDEA1, the heme-binding domain controls a phosphodiesterase domain that regulates the abundance of a cyclic nucleotide second messenger. A serendipitous discovery of apparent heme binding during the purification of NPAS2, a mammalian bHLH (basic helix-loop-helix)–PAS transcription factor, stimulated us to investigate whether NPAS2 might represent yet another heme-based mode of signal transduction by PAS domains.

Overexpression of a fragment of NPAS2 containing its bHLH DNA binding domain and both PAS domains in bacteria yielded amber-colored cells. The absorption spectra of liquid cultures containing those cells revealed a correlation between NPAS2 expression and heme protein absorption (Fig. 1A). Obvious peaks of absorption for the intact living cells were observed at 426 nm (Soret or gamma) and 561 nm (alpha). Upon centrifugation of a cell lysate, the bulk of overexpressed NPAS2 was recovered as an insoluble red suspension. The apoprotein resulting from solubilization of the material by denaturation and renaturation was easily reconstituted with free hemin (*14, 15*). The absorption peaks for the reconstituted proteins also occurred at 426 nm and 561 nm, with a lower extinction peak becoming detectable at 530 nm (beta) (Fig. 1B). To examine the stability and stoichiometry of the heme, we exposed this reconstituted material to a fivefold molar excess of $His^{64} \rightarrow Tyr$, $Val^{68} \rightarrow Phe$ apomyoglobin (apo-H64Y/V68F) (*16*). As indicated by the similar rates of apo-H64Y/V68F reconstitution with heme abstracted from either NPAS2 or *Bradyrhizobium japonicum* FixL, the heme stability of the two proteins was comparable (Fig. 1C). The final absorption value for the apo-H64Y/V68F treated with NPAS2 showed that NPAS2 had rough-

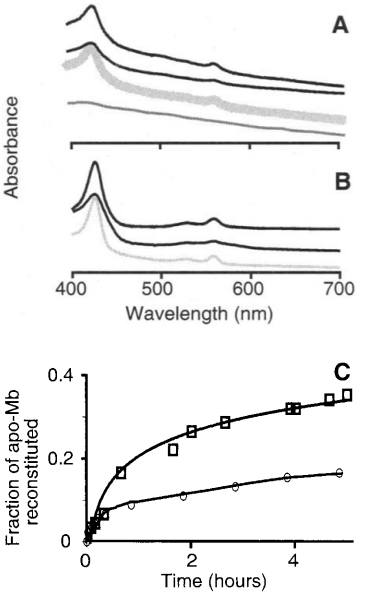

Fig. 1. Heme content and stability of holo-NPAS2. (**A**) Production of heme protein in whole *E. coli* cells after the induction of TG1 cells not expressing recombinant genes (thin gray line) or expressing the NPAS2 truncated recombinant forms bHLH–PAS-A–PAS-B (thick black line), bHLH–PAS-A (thin black line), or PAS-B (thick gray line). NPAS2 fragments, placed downstream from a tac promoter in a pUC19-derived expression vector, were expressed after 5 hours of isopropyl-β-D-thiogalactopyranoside induction in *E. coli* strain TG1. The absorption spectra of 10-fold concentrated cultures of intact cells were collected with an ATI Unicam UV-4 UV/Vis spectrophotometer (Spectronic Instruments Inc., Rochester, NY) containing a turbid-sample accessory. (**B**) Absorption spectra of the deoxy (Fe^{II}) forms of purified bHLH–PAS-A–PAS-B (thick black line), bHLH–PAS-A (thin black line), and PAS-B (gray line). Deoxy species were prepared by reducing the protein with dilute dithionite in an anaerobic glove box and rapidly transferring it, by gel filtration, to 0.10 M sodium phosphate (pH 7.5) and 5 mM dithiothreitol (DTT). (**C**) Extraction of heme from reconstituted holo-bHLH–PAS-A–PAS-B (squares) or from *B. japonicum* FixL protein (circles) by a fivefold molar excess of apo-H64Y/V68F sperm whale myoglobin at pH 6.5 and 25°C (*16*).

[1]Departments of Biochemistry and Plant Biology and Plant Biotechnology Center, The Ohio State University, 1060 Carmack Road, Columbus, OH 43210, USA. [2]Department of Biochemistry, University of Texas Southwestern Medical Center, 5323 Harry Hines Boulevard, Dallas, TX 75390, USA.

*To whom correspondence should be addressed. E-mail: steven.mcknight@utsouthwestern.edu, magg@biochem.swmed.edu

ly twice the heme content of *B. japonicum* FixL per monomer. We next extracted the heme from holo-NPAS2 with alkaline pyridine and quantitated the release of pyridine hemochrome (*17*). Consistent with the findings of the apo-myoglobin competition experiment, this experiment revealed 1.7 moles of heme per mole of NPAS2.

The presence of two hemes per monomer of NPAS2 suggested that each of its two PAS domains was binding heme. To test this idea, we prepared derivatives of NPAS2 that contained only the PAS-A or PAS-B domain (*18*). The absorption spectra of intact cells expressing these variants were immediately recognizable as heme protein spectra (Fig. 1A). Interestingly, the deoxy spectra of both purified PAS-A and PAS-B exhibited hemochrome absorption spectra characteristic of heme-iron hexacoordination (Fig. 2).[5] Typical absorption spectra of proteins, such as FixL, that contain pentacoordinate heme iron in their unliganded ferrous forms have a broader Soret peak around 434 nm and a single, broad band of lower extinction around 556 nm (*19*). In contrast, PAS-A and PAS-B spectra have a sharp Soret peak (426 nm) and well-resolved alpha (561 nm) and beta (530 nm) bands in the far-red region, with the alpha peak having greater extinction than the beta peak (Fig. 2). These features resemble the deoxy spectra of two bacterial gas sensors: the direct oxygen sensor protein *Ec*Dos of *Escherichia coli* and the CO-sensor protein CooA of *Rhodospirullum rubrum* (*20, 21*). Both are known to contain heme iron coordinated to protein side chains at both axial positions (*22, 23*).

A heme-based sensor is defined as a protein in which a heme-binding domain controls the activity of another domain in the protein (*19*). To test whether DNA binding by the bHLH domain was coupled to the state of one or both hemes in NPAS2, we examined the effect of CO on binding of NPAS2 to DNA. Unlike other heme ligands such as oxygen or nitric oxide, CO does not interact with heme proteins except through the iron atom. Therefore, any effects of CO on the bHLH domain can only be the result of coupling to the heme-binding domain. As an additional control, the effect of CO on DNA binding of NPAS2 lacking heme (apo-NPAS2) was determined.

Binding of CO to the various heme-containing truncations of NPAS2 was easily followed spectroscopically because of the pronounced differences between the spectra of the deoxy and CO derivatives (Fig. 2). The equilibrium dissociation constants (K_d) for binding of CO, obtained from direct titrations with CO, were 1 to 2 μM for NPAS2 and PAS-A, and 21 μM for PAS-B. Individual time courses for the association of CO to NPAS2 fit two exponentials (Fig. 3),[5] with each term contributing equally to the total absorbance change. These data indicated that the two rates might reflect ligand binding to each of the two hemes in holo-NPAS2. Consistent with this interpretation, experiments with the isolated PAS-A and PAS-B derivatives revealed that CO bound to each heme at a single rate matching only one of the two components of the holo-NPAS2 rate curve (Fig. 3). At CO concentrations below 80 μM, the rates of CO association to the three proteins increased linearly in proportion to ligand concentration. On the basis of this linear portion of the curve, the association rate constant for binding of CO to the bHLH–PAS-A derivative (k_{on} = 0.37 μM^{-1} s^{-1}) was greater than that for CO binding to the PAS-B variant (k_{on} = 0.04 μM^{-1} s^{-1}) by a factor of ~10. At higher CO concentrations, the observed rates of ligand association approached a limiting value of 70 s^{-1} for bHLH–PAS-A and 7 s^{-1} for PAS-B. The phenomenon of limiting rates in displaceable-residue heme proteins is known to reflect the equilibrium between hexacoordinate and pentacoordinate states and indicates a relatively slow conversion of the heme iron from a hexacoordinate state inaccessible to ligand to an accessible pentacoordinate state (*20, 22, 24*).

The functional consequences of heme and CO binding were probed by in vitro DNA binding assays. Sequence-specific DNA binding by NPAS2 depends on the availability of BMAL1, its obligate heterodimeric partner, and the ratio of the reduced and oxidized forms of nicotinamide adenine dinucleotide phosphate (NADPH and NADP, respectively) (*25*). Both apo-NPAS2 and holo-NPAS2 bound DNA only in the presence of BMAL1 (Fig. 4, B and C; lane 6). Both holo- and apo-NPAS2 required high NADPH/NADP ratios to bind DNA, hence the response to this redox signal does not require heme (Fig. 4, B and C; lanes 1 to 6). Only holo-NPAS2 responded to CO addition (Fig. 4, B and C; lanes 7 to 10). Up to 30 μM

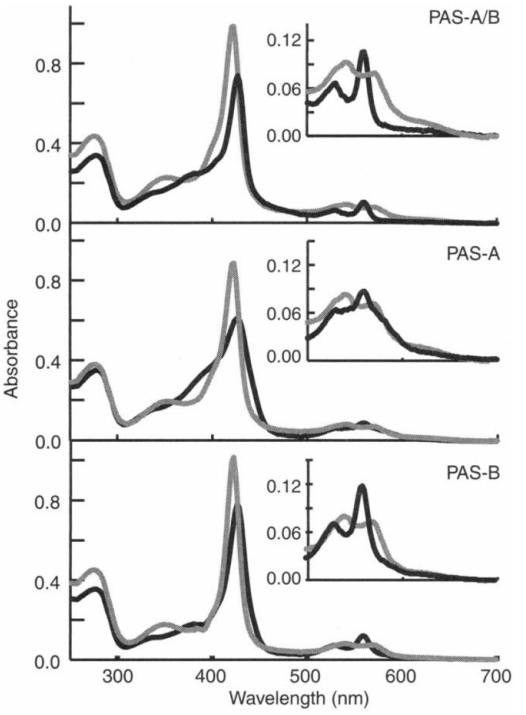

Fig. 2. Binding of carbon monoxide to ferrous forms of NPAS2. Absorption spectra are shown for the bHLH–PAS-A–PAS-B, bHLH–PAS-A, and PAS-B truncations before (deoxy forms, black lines) and after (CO-bound forms, gray lines) addition of ~1 atm of CO at pH 7.5 and 23°C to samples in stoppered quartz cuvettes inside an anaerobic glove box. The samples contained ~10 μM heme.

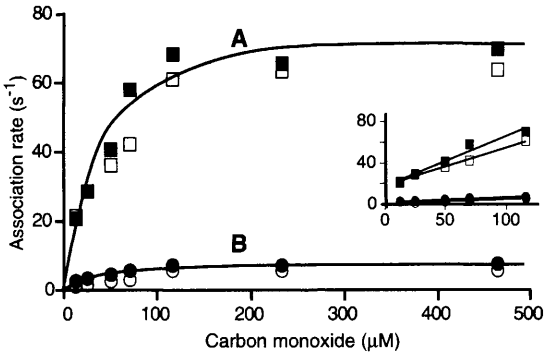

Fig. 3. Rates of association of carbon monoxide to NPAS2. Observed rates of CO association to the bHLH–PAS-A (open squares) and PAS-B (open circles) regions of NPAS2 are compared with the rates of CO association calculated by deconvoluting two exponentials from kinetic traces measured for bHLH–PAS-A–PAS-B (closed symbols). Rates of ligand association at 25°C were measured for 1 to 8 μM deoxy protein mixed with 12 to 480 μM CO prepared in the same buffer [0.10 M sodium phosphate (pH 7.5) and 5 mM DTT]. The protein and CO solutions were mixed in a stopped-flow spectrometer (Applied Photophysics Ltd., Leatherhead, UK), and association of CO was followed at 424 nm. Association rate constants for CO binding were estimated from the linear portion of the curves (A, PAS-A; B, PAS-B) at low concentrations of CO (inset).

CO had no effect on DNA binding by apo-NPAS2, whereas CO concentrations above 3 μM abolished DNA binding by holo-NPAS2. The titration curve for CO binding to holo-NPAS2 closely matched the titration curve for inhibition of DNA binding (Fig. 4A; Fig. 4C, lanes 7 to 10). Thus, heterodimer formation and DNA binding can be blocked by a heme-mediated mechanism or by an independent inhibition that results if the NADPH/NADP ratio is too low. If either or both signals that inhibit formation of the NPAS2-BMAL1 heterodimer are present, then the unproductive BMAL1-BMAL1 homodimer is formed.

These experiments provide evidence that the mammalian transcription factor NPAS2 binds heme as a prosthetic group to form a gas-regulated sensor. It was essential to use CO to establish unambiguously the coupling of heme state to DNA binding, because NPAS2 has a separate redox-sensing activity that might be perturbed by oxygen (O_2) or nitric oxide (NO). Having established that NPAS2 is a heme-based sensor, it is now of great interest to determine which heme ligand(s) is sensed by NPAS2 in vivo. Both O_2 and NO have been established as signals for other heme-based sensors. However, the NPAS2 derivatives in our study failed to react with NO (except at super-physiological concentrations) and reacted irreversibly with O_2 (*26*). If native NPAS2 is similarly reactive, it seems unlikely that either O_2 or NO is the natural ligand.

Our in vitro experiments have identified CO as a reasonable candidate ligand for NPAS2. This raises two questions. First, could CO ever be present in cells at levels sufficient to inhibit NPAS2-BMAL1 DNA binding activity? Ronnett and colleagues estimate that CO concentrations in several types of neuronal cells range from 3 to 30 μM, which would be sufficient to regulate NPAS2 (*27*). Second, why might NPAS2 have evolved as a CO-sensitive transcription factor? Like the transcription factor Clock, NPAS2 regulates gene expression as a function of the day-night cycle (*28*). NPAS2 and Clock are similar in primary sequence, share the same dimeric partner (BMAL1), and bind DNA in a manner dependent on intracellular redox potential (*25*). NPAS2 knockout mice fail to exhibit rhythmic *Per2* gene expression in regions of the forebrain that are known to express NPAS2 (*28*). These same regions of the forebrain exhibit enhanced expression of the gene for heme oxygenase 2 (HO-2), an enzyme that generates CO using heme as a substrate (*29*). A hypothetical means of reciprocally connecting CO production to the regulatory system controlling circadian rhythm is suggested by recent DNA microarray studies (*30*). Peak expression of aminolevulinic acid synthase (ALAS), the rate-limiting enzyme for heme biosynthesis, occurs at the beginning of the active, nocturnal period of the rodent circadian cycle. If oscillatory expression of ALAS mRNA were to direct a corresponding oscillation in heme biosynthesis, then heme catabolism by HO-2 to generate CO might also vary as a function of the day-night cycle. If so, the role of the NPAS2-BMAL1 heterodimer in orchestrating circadian oscillation of metabolic pathways, including heme biosynthesis, might be reciprocally linked to heme catabolism by the molecular sensor described here.

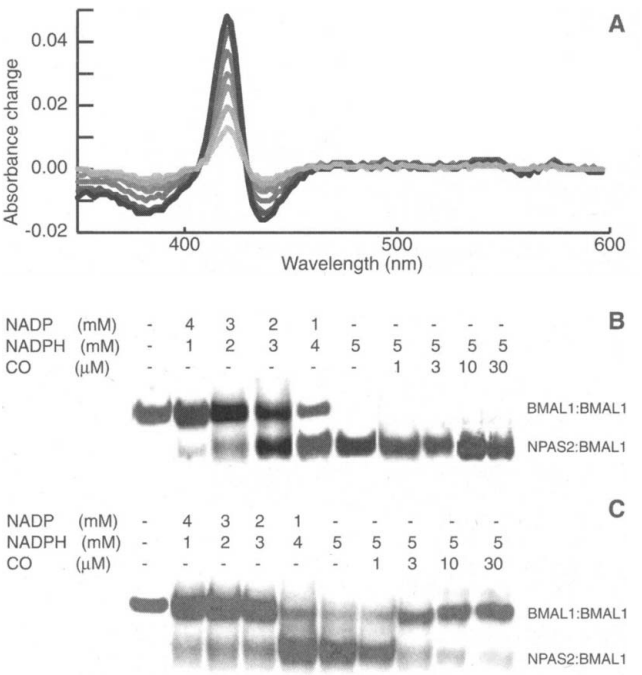

Fig. 4. Influence of heme, CO, and NADPH on sequence-specific DNA binding by NPAS2-BMAL1 heterodimers. (**A**) Difference spectra resulting from a direct titration of the deoxy form of bHLH–PAS-A–PAS-B (0.1 μM) with 1, 2.5, 5, 6, 7, 8, 10, and 12 μM CO (light gray to dark gray) at pH 7.5 and 25°C in a cuvette (path length 5 cm), as monitored with an ATI Unicam UV-4 UV/Vis spectrophotometer. Proportions of liganded and unliganded species were calculated from decomposition of entire (350 to 700 nm) absorption spectra by multiple linear regression analysis. (**B** and **C**) Electrophoretic mobility shift assays of a ^{32}P-labeled double-stranded DNA response element (NRE) resulting from addition of BMAL1 and either apo-NPAS2 (B) or holo-NPAS2 (C), varying NADPH/NADP ratios, and varying concentrations of CO. Gel mobility shift assays were essentially as described (*25*), except that all manipulations were done inside an anaerobic glove box. Protein (0.5 μg of NPAS2 plus 1 μg of BMAL1) was incubated with 200 nM ^{32}P-labeled NRE having the sequence 5′-AGGGGCGC-CACGTGAGAGGCCT-3′ in 10 mM Hepes (pH 7.5), 50 mM NaCl, 0.5% *n*-octyl glycoside, 2 mM DTT, bovine serum albumin (0.12 mg/ml), 1.2 mM $MgCl_2$, and polydeoxyinosine-deoxycytidine (0.05 mg/ml). Heme status was verified by monitoring the absorption of the reaction mixtures at the start and conclusion of reactions.

References and Notes

1. E. C. Hoffman *et al.*, *Science* **252**, 954 (1991).
2. B. L. Taylor, I. B. Zhulin, *Microbiol. Mol. Biol. Rev.* **63**, 479 (1999).
3. M. A. Gilles-Gonzalez, G. S. Ditta, D. R. Helinski, *Nature* **350**, 170 (1991).
4. W. D. Hoff *et al.*, *Biochemistry* **33**, 13959 (1994).
5. J. M. Christie, M. Salomon, K. Nozue, M. Wada, W. R. Briggs, *Proc. Natl. Acad. Sci. U.S.A.* **96**, 8779 (1999).
6. S. Hill, S. Austin, T. Eydmann, T. Jones, R. Dixon, *Proc. Natl. Acad. Sci. U.S.A.* **93**, 2143 (1996).
7. M. S. Denison, A. Pandini, S. R. Nagy, E. P. Baldwin, L. Bonati, *Chem. Biol. Interact.* **146**, 3 (2002).
8. U. K. Genick *et al.*, *Science* **275**, 1471 (1997).
9. W. Gong *et al.*, *Proc. Natl. Acad. Sci. U.S.A.* **95**, 15177 (1998).
10. J. H. Morais-Cabral *et al.*, *Cell* **95**, 649 (1998).
11. S. Crosson, K. Moffat, *Proc. Natl. Acad. Sci. U.S.A.* **98**, 2995 (2001).
12. C. A. Amezcua, S. M. Harper, J. Rutter, K. H. Gardner, *Structure* **10**, 1349 (2002).
13. M. A. Gilles-Gonzalez, *IUBMB Life* **51**, 165 (2001).
14. F. Ascoli, M. R. Rossi-Fanelli, E. Antonini, *Methods Enzymol.* **76**, 72 (1981).
15. The insoluble fraction of cell lysates was clarified with 0.5% SDS, which was then removed by KCl precipitation. Gel filtration (Sephacryl S-200) and anion-exchange (DEAE-sephacel) chromatography yielded ~90% pure NPAS2 apoprotein. This protein [~20 μM apo-protein in 0.10 M sodium phosphate, 15% v/v glycerol, and 0.1 mM EDTA (pH 7.5)] was titrated with 2 mM hemin in 10 mM NaOH. The resulting holo-protein was transferred to 0.10 M sodium phosphate, 15% v/v glycerol, and 0.1 mM EDTA (pH 7.5) by gel filtration (Sephacryl S-200).
16. M. S. Hargrove *et al.*, *J. Biol. Chem.* **269**, 4207 (1994).
17. C. A. Appleby, in *Methods for Evaluating Biological Nitrogen Fixation*, F. J. Bergerson, Ed. (Wiley, New York, 1980), pp. 315–335.
18. All three NPAS2 species in this study were truncated forms of the native NPAS-2 protein. They were as follows: bHLH–PAS-A–PAS-B, residues 1 to 416; bHLH–PAS-A, residues 1 to 246; and PAS-B, residues 160 to 346.
19. M. A. Gilles-Gonzalez *et al.*, *Biochemistry* **33**, 8067 (1994).
20. V. M. Delgado-Nixon, G. Gonzalez, M. A. Gilles-Gonzalez, *Biochemistry* **39**, 2685 (2000).
21. D. Shelver, R. L. Kerby, Y. He, G. P. Roberts, *Proc. Natl. Acad. Sci. U.S.A.* **94**, 11216 (1997).
22. G. Gonzalez *et al.*, *Biochemistry* **41**, 8414 (2002).
23. W. N. Lanzilotta *et al.*, *Nature Struct. Biol.* **7**, 876 (2000).
24. M. S. Hargrove, *Biophys. J.* **79**, 2733 (2000).
25. J. Rutter, M. Reick, L. C. Wu, S. L. McKnight, *Science* **293**, 510 (2001).
26. E. M. Dioum *et al.*, data not shown.
27. T. Ingi, G. Chiang, G. V. Ronnett, *J. Neurosci.* **16**, 5621 (1996).
28. M. Reick, J. A. Garcia, C. Dudley, S. L. McKnight, *Science* **293**, 506 (2001).
29. S. R. Vincent, S. Das, M. D. Maines, *Neuroscience* **63**, 223 (1994).
30. B. H. Zheng *et al.*, *Cell* **105**, 683 (2001).

31. We thank M. S. Hargrove and J. S. Olson for H64Y/V68F sperm whale myoglobin and R. W. Estabrook and J. A. Peterson for helpful discussions. Supported by NIH grants R01 HL640381 (M.-A.G.-G.) and NIH5-T32-GM08-291-12 (J.R.), NIMH grant R01 MH5938805 (S.L.M.), and unrestricted funds from an anonymous donor.

16 September 2002; accepted 26 October 2002
Published online 21 November 2002;
10.1126/science.1078456
Include this information when citing this paper.